High density aromatic peptides protect retinal ganglion cells in mouse retina following optic nerve crush injury.

Margaret A. MacNeil [1,2], Virginia Garcia-Marin [1,2], Alexander Birk[1]

[1]Department of Biology, York College of the City University of New York, Jamaica, NY 11451

[2]Department of Biology, CUNY Graduate Center, New York, NY

Running title: Protection of RGCs with HDAP2

Keywords: optic nerve crush; retinal ganglion cells; glaucoma; neural trauma; Müller cells

Corresponding author:

Margaret A. MacNeil, Ph.D.

York College, CUNY

Department of Biology, 94-20 Guy R. Brewer Blvd.

Jamaica, NY 11451

Phone: 718-262-2711

Fax: 718-262-2369

mmacneil@york.cuny.edu

Support: This work was supported by a grant from PSC-CUNY grant #642000-00-52 (M.A.M.). and funding from Social Profit Network (A.B.).

Abstract

Purpose: Mitochondrial dysfunction plays a significant role in the death of retinal ganglion cells (RGCs) and their axons in retinal neurodegenerative diseases. We studied the effect of the mitochondrial-targeted HDAP2 (High Density Aromatic Peptide 2) to protect MDBK cells following serum starvation in cultured cells, and in mouse retinal ganglion cells following optic nerve crush.

Methods: Uptake, toxicity, and efficacy of HDAP2 was studied in cultured cells under conditions of serum starvation. Once preliminary safety and efficacy of the peptide was established *in vitro*, HDAP2 was administered to mice following unilateral optic nerve crush and the distribution and survival of RBPMS-labeled RGCs was assessed.

Results: We found that water-soluble HDAP2 localizes to mitochondria and improves the mitochondrial membrane potential, prevents oxidative stress, and reduces death of cells grown in serum-free culture media. In mice treated systemically with biotinylated peptide, we found that HDAP2 labeled all layers of the retina in a pattern similar to the mitochondrial marker Cox IV, and that the peptide was colocalized with retinal ganglion cells and Müller glia. Animals treated with HDAP2 following optic nerve crush showed significantly greater survival of retinal ganglion cells compared to untreated animals at all retinal eccentricities.

Conclusion: Our results demonstrate that HDAP2 protects cells against serum starvation-induced decreases in mitochondrial membrane potential and leads to significant protection of retinal ganglion cells in the mouse retina following optic nerve crush *in vivo.* These results suggest that therapeutic agents preserving the mitochondrial membrane potential may help protect neurons following trauma or from neurodegenerative disease.

Introduction

Degeneration of retinal ganglion cells and their axons is a hallmark of many optic neuropathies including glaucoma, traumatic optic neuropathy, and diabetic retinopathy (Jassim et al., 2021; Nickells et al., 2012; Williams et al., 2020). The exact cause of the degeneration is unknown, but likely results from multiple factors, including aging (Hou et al., 2022; Samuel et al., 2011), loss of neurotrophic factors (Almasieh et al., 2012), axon transport disruption (Crish et al., 2010), and mitochondrial dysfunction (Schrier & Falk, 2011).

Retinal ganglion cells (RGCs) are particularly vulnerable to neuropathy because they are among the most highly metabolically active cells in the body (Liu & Prokosch, 2021). Large amounts of ATP are needed to support synaptic activity on dendritic arbors, to transport organelles and neurotrophic factors along axons, and to maintain the cellular resting potential, particularly in unmyelinated intraretinal fibers in the vicinity of the optic disk (Wilkison et al., 2021). RGCs are supported by an abundance of mitochondria, which are most densely concentrated in parts of the cell experiencing the greatest energy need (Barron et al., 2004; Yu Wai Man et al., 2005). The function of RGCs is impaired when energy production within mitochondria is disrupted, which leads to synaptic pruning, dendritic atrophy, axon degeneration and cell loss (Ito & Polo, 2017; Kong et al., 2009).

Treatments aimed to protect mitochondria also seem to protect RGCs and their axons. Oral administration of vitamin B3, a precursor of nicotinamide adenine dinucleotide (NAD), improved mitochondrial function and prevented progression of glaucoma in aged mice (Williams et al., 2017), and increased mitochondrial size and motility following experimentally induced optic hypertension (Tribble et al., 2021).

Simply transplanting healthy mitochondria into the vitreous following ONC increases survival of RGCs and the number of axons growing through the crush site (Nascimento-Dos-Santos et al., 2020). Because RGCs have high numbers of mitochondria, therapeutic agents that support mitochondria may remedy multiple factors contributing to these neurodegenerative processes and improve RGC survival (Chrysostomou et al., 2013; Lin & Beal, 2006; Murphy, 2016; Nunnari & Suomalainen, 2012).

In this paper we report on the neuroprotective effects of a novel high-density aromatic peptide (HDAP2). The core of HDAP2 consists of a Phe-Phe dipeptide, which promotes formation of electroconductive hydrophobic domains that optimizes the mitochondrial membrane potential to limit dysfunctional mitochondria-mediated oxidative stress. Our results suggest that HDAP2 targets mitochondria and can protect cells against serum starvation of cells in culture and leads to significant protection of retinal ganglion cells in mouse retina at two weeks following optic nerve crush.

Methods

Peptide

We have designed a novel, high density aromatic peptide (HDAP2, patent-pending with the Research Foundation, City University of New York) that stabilizes mitochondrial function and optimizes the mitochondrial membrane potential. The peptide was synthesized commercially (96.2% pure; GenScript, Piscataway, NJ) and mass spectrometry results, HPLC purity, appearance and gross weight were all consistent with specifications.

Tissue Culture Experiments

Cells and media

Tissue culture studies were carried out using Madin-Darby Bovine Kidney (MDBK) cells (Lot ATCC-CCL22) derived from primary tissue. MDBK cells were plated and grown in Dulbecco's Modified Eagle's Minimum Essential Medium (DMEM, Cytiva) with 4.5 g of glucose and 10% horse serum, and held in an incubator with 5% CO_2 at 37 °C.

HDAP2 uptake

To assess uptake of HDAP2 into cells, cultures were incubated in serum-free media for three days to deplete endogenous biotin (Birk et al., 2013) and then treated with biotinylated HDAP2 (1 μM) for one hour. Cells were fixed with 4% paraformaldehyde and incubated for one hour with Alexa Fluor 594 conjugated streptavidin (1:100, Jackson ImmunoResearch) to localize the peptide within the cells, Hoechst 33342 (10 μg/ml, Novus) to label nuclei, and Mito Tracker Red CMXRos (MTR; 50 nM, Invitrogen) to identify mitochondria; MTR binds to thiol groups, which are heavily concentrated in the mitochondrial matrix. Cells were rinsed and imaged immediately in the dish using a Nikon Eclipse 50i fluorescent microscope with a 40X immersion objective (NA 0.8).

Serum starvation experiments

We wanted to assess HDAP2's ability to improve cell viability and function following serum starvation. For all experiments, MDBK cells were seeded in 35 mm cell culture dishes (5 X 10^4 cells) in DMEM medium with 10% FBS (Fetal Bovine Serum) for

24 hrs and then incubated in serum-free medium with or without HDAP2 (1 μM) for 5 days to induce cell death. For quantitative measurements, wells were washed to remove dead cells, and then stained with alamarBlue (Mazzio & Soliman, 2004) for 60 min. Quantitative analysis of dye conversion was measured using a fluorescent plate reader (550 ex/580 em) and cell viability was expressed as folds change (increase or decrease) over serum-starved untreated cells.

To measure the effects of HDAP2 on the mitochondrial potential and cellular oxidative stress, cells were cultured in DMEM/F12 without fetal bovine serum (FSB) in the presence or absence of HDAP2 (1 μM). After 3 days, nuclei were labeled with Hoechst 33342 (10 μg/ml) and cells were incubated for 15 minutes at 37°C with MTR (100 nM) to evaluate the strength of the mitochondrial potential or were incubated with the general oxidative stress indicator CM-H2DCFDA (5 μM, Invitrogen, Carlsbad, CA) for 15 min at 37°C. In each instance, cells were imaged immediately after staining and prior to fixation.

Unless otherwise noted, data for all tissue culture experiments were collected from three independent trials, with each experiment done in triplicate. For each experiment, 4-6 fields of cells were randomly selected and imaged using a Nikon Eclipse 50i fluorescent microscope with a 40X immersion objective (NA 0.8) and using filters specific for either green or red wavelengths as appropriate (ex488nm/ex515-540nm). Photooxidation of the indicator dyes were minimized by using single exposures to the fluorescence for each field imaged. Fluorescence intensity was analyzed using ImageJ (NIH), and MTR and CM-H2DCFDA fluorescence were normalized to Hoechst fluorescence to account for differences in cell number in each field. Differences among

groups were compared by Student's t-test and *P* values less than 0.05 were considered significant. All data are expressed as means ± SEM.

Animal Experiments

We studied adult C57BL/6 mice (The Jackson Laboratory, Bar Harbor, ME) of either sex, 2-6 mos. of age that were bred and housed in the animal facility at York College, CUNY. All procedures using animals were approved by the York College IACUC and were consistent with the ARVO Statement for the Use of Animals in Ophthalmic and Vision Research.

HDAP2 uptake in retina

Adult animals were injected with 50 mg/kg biotinylated HDAP2 (IP; GenScript, Piscataway, NJ) reconstituted in saline and observed for 2 hours before sacrifice. Eyes were marked to record their orientation, and the animals were given an overdose of ketamine (300 mg/kg) / xylazine (60 mg/kg) (IP) before removing each eye from the orbit with forceps. Whole eyes were dropped into 4% paraformaldehyde that was constituted in either 0.1M Tris or phosphate buffers (pH 7.3) and after ten minutes, the cornea, lens and vitreous body were removed to ensure better penetration of the fixative into the retina. The eyecups were returned to the fixative for one hour. Retinas for wholemounts were dissected from the pigment epithelium by cutting along the ora serrata, gently teasing the retina away from the back of the eye and then freeing the retina by severing the optic nerve. Retinas for cryo-sectioning remained in the eyecup, were cryoprotected in 0.1M Tris or phosphate-buffered sucrose (10%, 20% and 30%) prior to embedding in OCT (Polyfreeze, Polysciences) and sectioned at a thickness of

14 μm at -25° C using a cryostat (Leica CM3050S). Uptake of HDAP2 was revealed by incubating the tissue (wholemounts and sections) with Alexa Fluor-conjugated streptavidin (1:200, Jackson ImmunoResearch) either overnight (sections) or for three days (wholemounts) and counterstained with various antibodies (described below).

Optic Nerve Crush Procedure

Adult mice (2-6 mo.) were anesthetized with a cocktail of ketamine (85 mg/kg) and xylazine (20 mg/kg) (IP), the corneas were numbed with a drop of 0.5% proparacaine hydrochloride ophthalmic solution (Falcon Pharmaceuticals) and the animals were positioned under a Nikon dissecting microscope, dorsolaterally either on the left or right sides. The dorsomedial conjunctiva was cut with microdissection spring scissors, the intraocular muscles were separated, and the eyeball was slightly retracted to expose the optic nerve. Fine, self-closing forceps (Roboz, RS-5027) were used to clamp the optic nerve 1-2 mm behind the globe, for approximately 3 seconds (Kalesnykas et al., 2012; Tang et al., 2011) without applying additional tension. The eye was repositioned within the orbit, the conjunctiva reflected over the extraocular eye muscles and the incision covered with ophthalmic polymyxin B-neomycin-bacitracin ointment (3.5 mg/gm, Bausch and Lomb). The optic nerves from the contralateral eye were untouched and used as untreated controls. Following the crush procedure, mice were given a subcutaneous injection of extended-release buprenorphine (0.05 mg/kg, Ethiqua XR) for analgesia and placed on a heating pad until awake and grooming, at which point they were returned to their home cages. Half the animals were given HDAP2 immediately following the procedure and then daily thereafter (3 mg/kg, IP) for 14 days.

Immunohistochemistry

Fixed retinas were labeled with cell markers using conventional immunohistochemical protocols to identify cells and structures associated with HDAP2, and to identify retinal ganglion cells and starburst amacrine cells to assess cell survival following optic nerve crush. Retinas and sections were blocked and permeabilized with 4% normal donkey serum in 0.1M Tris or phosphate buffers with 0.5% Triton-X for 1 hour and then incubated overnight (for sections) or for 3 days (for wholemounts) at 4°C in selected primary antibodies, and 2% normal donkey serum in the same buffer. The tissue was rinsed 3 X 10 minutes with buffer and then incubated with secondary antibodies for one hour at room temperature (sections) or overnight at 4° C for wholemounts. Antibodies and markers used were rabbit anti-RBPMS (1:200; Invitrogen, PA5-31231) to label all retinal ganglion cells; goat anti-choline acetyltransferase (ChAT 1:100; EMD Millipore, AB144P) to label starburst amacrine cells; rabbit anti-glutamine synthetase (1:200; Invitrogen, PA1-46165) to label Müller cells; and rabbit anti-cox4 (1:200; Invitrogen, PA5-29992) to identify mitochondria. Secondary antibodies were raised in donkey and conjugated with either Alexa Fluor 488, 594 or 647 (1:500, Life Sciences). To identify the distribution of cell nuclei, and to delineate retinal layers, tissue was labeled with the nuclear stain ToPro3 (1:1000; Invitrogen) for 15 minutes. After staining, sections and retinas were rinsed in buffer and coverslipped in Vectashield mounting media (Vector Labs) to prevent photobleaching.

Imaging and Data Analysis

Retinal cells were imaged using an Olympus Fluoview 300 confocal microscope with an Olympus 40 X oil immersion objective (NA 1.0) in dorsal, ventral, nasal and

temporal regions of the retina at each of three eccentricities approximately 1, 2 and 3 mm from the optic disk. The laser intensity for the green channel was set at ~530V so that RBPMS expression could be compared between treatment conditions. In central regions, Z-stacks (1 μm steps) were collected through the ganglion cell layer to ensure that RGCs above and below the middle focal plane were imaged and a through focus projection was generated and used to count cells. In midperipheral and peripheral areas of the retina, single images were collected instead because cells in the ganglion cell layer were visible in a single focal plane. Each site was imaged separately using each of three wavelengths (488, 594, and 647) and then merged in Photoshop to observe RGCs, starburst cells and cell nuclei in the same fields. Labeled cells in each image field (350 μm X 350 μm) were counted manually using ImageJ (NIH) while blinded to the experimental condition and used to compute the densities of RGCs and the ratios of RBPMS to ChAT cells for each location and condition. RBPMS expression in the tissue was quantified using the "Analyze" feature in ImageJ to compute the mean pixel intensity (in arbitrary fluorescence units) from the confocal images.

Statistics

Mean values for each treatment and eccentricity were compared and tested for significance using either a Student's t-test or one-way analysis of variance (ANOVA) with graphing and statistical software (GraphPad Prism, GraphPad Software). *P* values less than 0.05 were considered significant and all data are expressed as means ± SEM.

Results

HDAP2 is non-toxic to cells in culture and has no observable adverse effects in mice

Cellular toxicity was assessed in cultured cells by incubating MDBK cells in dilutions of HDAP2, up 100 μM. No toxicity in MDBK cell growth was observed (data not shown). Toxicity in mice was tested by administering treatment doses (3 mg/kg) daily to animals for 14 days (n>40) or biweekly for two months (n=4) with no adverse effects. None of the animals died, all exhibited normal grooming behaviors and maintained their original weights. Post-mortem analysis of retinal tissue in control eyes showed normal retinal anatomy, without obvious signs of neuronal death, altered mosaics of retinal ganglion cells or disruptions to lamination patterns (Figures 2-4). Thus, prolonged treatment with HDAP2 had no detectable toxic effects on the health of mice or damage to the retina.

HDAP2 co-localizes with mitochondrial markers in cultured cells and improves cell survival following serum starvation

Cultured MDBK cells that were either incubated with HDAP2 or maintained in control media, were labeled with Hoechst and Alexa Fluor 488 conjugated streptavidin to evaluate the distribution of biotin, either endogenous to the cells or bound to HDAP2. In both conditions, Hoechst-positive cell nuclei were clearly visible, but only cells incubated with HDAP2 showed an extensive network of perinuclear streptavidin labeling within the cells, demonstrating extensive uptake (Figure 1A). Endogenous biotin in the control cells was detectable with streptavidin, but the intensity of fluorescence was significantly weaker than in cells with biotinylated HDAP2 (n= 4; P<0.001) (Figure 1B). When cells were incubated with both biotinylated HDAP2 and MTR, a mitochondria potential marker dye that identifies both living and fixed mitochondria, the two markers

were colocalized (gray-green color), indicating that HDAP2 targets mitochondria (Figure 1C).

HDAP2 protects the mitochondrial membrane potential and prevents oxidative stress following serum starvation

Serum starved MDBK cells were used to evaluate the protective effect of HDAP2 on mitochondria and cell survival. Co-incubation of HDAP2 (1 μM) with MDBK cells in serum-free conditions for 3-4 days increased the mitochondrial membrane potential in cells by 150% compared to values recorded in control cells in serum-free conditions ($P<0.0001$) (Figure 1D). In addition, HDAP2-treated cells showed significant reductions in CM-H2DCFDA fluorescence, indicating decreased cellular oxidative stress (>80%; $P<0.0001$) (Figure 1E) and overall increased cell survival by 50% ($P<0.001$) (Figure 1F) compared to untreated controls when MDBK cells were grown in serum-free conditions for 5 days,

Distribution of HDAP2 peptide in the retina

Systemic administration of biotinylated HDAP2 in mice (3 mg/kg, IP) labeled all layers of the retina, at levels exceeding endogenous biotin (Figure 2A). Since HDAP2 colocalizes with mitochondrial membranes, we labeled retinal sections with antibodies against the mitochondrial CoxIV for comparison. HDAP2 was uniformly distributed throughout the plexiform layers, and matched the pattern of CoxIV labeling, suggesting that HDAP2 is localized within mitochondria-dense regions of the retina. Vertical and tangential sections through the ganglion cell layer showed heavy HDAP2 labeling in Müller cell end feet (Figure 2B) and elevated labeling in RGC somas and axons, where

mitochondria are in high density (Wang et al., 2003).

Quantification of Retinal Ganglion Cell Survival

To test whether the protective effects of HDAP2 in serum-starved cultured cells extended to neurons *in vivo*, we studied the survival of RGCs following optic nerve crush (ONC) in the presence and absence of the peptide. To control for density differences of RGCs across the retina, we standardized values by comparing ratios of RBPMS-labeled RGCs (Mead et al., 2014) with the densities of starburst amacrine cells labeled by choline acetyltransferase (ChAT). Starburst amacrine cells, like other displaced amacrine cells, are unaffected by ONC in the short-term (Jakobs et al., 2005; Nadal-Nicolás et al., 2015). In control tissue, displaced starburst amacrine cells accounted for about 40% of cells in the ganglion cell layer and ratios of RBPMS labeled cells to ChAT neurons was about 4 to 1 in central retina and 3 to 1 at other eccentricities (Figure 3B). Following ONC, the mosaics of ChAT labeled neurons were not altered by the injury (Figure 3A) and the density of ChAT cells measured in control, ONC and HDAP2 conditions were not significantly different from each other ($P>0.05$, n=11-15 samples per eccentricity) (Figure 3C), demonstrating their usefulness as an internal control.

HDAP2 protects RGCs following ONC

Crushing the optic nerve resulted in the death of 85% of RGCs within 14 days of the injury (Figures 4 and 5), which is consistent with other studies (Duan et al., 2015; Galindo-Romero et al., 2011). In control retinas, the density of RBPMS labeled RGCs decreased predicably from center to periphery (Table 1, 4465 ± 106 cells/mm^2 to 2107 ±

126 cells/mm^2) (Table 1) and the average ratio of RGCs to starburst amacrine cells was about 3.3 to 1 (Figures 3B and 5A). After ONC, the density of RGCs decreased by about 85% (Table 1) and the average ratios of RBPMS to ChAT cells fell to 0.51 to 1 (Figures 4 and 5A). RBPMS expression in the tissue also decreased by a similar amount (Figure 5B). In contrast, ONC animals that were treated daily with HDAP2 had 40% more RBPMS labeled cells than untreated animals (Table 1), the expression of RBPMS doubled (9.8 $\pm$ 0.78 (treated) vs 4.4 $\pm$ 0.45 (untreated); $P<0.0001$, n=23) (Fig. 5B) and ratios of RGCs to ChAT cells were significantly higher compared to untreated ONC controls (0.70 to 1 vs 0.51 to 1, $P<0.001$, n=4 for each location) (Figure 5C).

Treatment with HDAP2 improved survival of RGCs at all eccentricities studied, but survival improved with increasing distance from the center; in central retina, the percent increase in RBPMS labeled cells was 18%, in midperipheral retina it was 38%, and in the periphery, the numbers of RBPMS-labeled cells was 50% greater than untreated ONC control retinas (Figure 5C).

Discussion

We have demonstrated that the novel peptide, HDAP2, supports mitochondrial function in cells affected by serum-starvation induced oxidative stress and protected RGCs *in vivo* following optic nerve crush injury.

HDAP2 peptide

HDAP2 is a novel synthetic peptide with a core of Phe-Phe (dArg-Phe-Phe-dArg-amide). The Phe-Phe dipeptide promotes formation of electroconductive hydrophobic domains, which optimizes electron transport (Marchesan et al., 2015; Nathanael et al.,

2018; Tao et al., 2017). However, previous targeting of mitochondria with short peptides containing the Phe-Phe motif resulted in mitochondrial toxicity and cell death (Jeena et al., 2017). The novel, high density aromatic peptide used in this study brackets Phe-Phe between two Arginine amino acids, to make HDAP2 both water soluble and non-toxic. . The addition of arginine provides overall positive charge to the HDAP2 analog, which is thought to be important for cell-permeability of peptides and their targeting into mitochondria (Zhao et al., 2004). Moreover, this new analog was amidated at the C-terminal and had both biotin and D-Arg to protect it against proteolytic degradation. Biotin on the N-terminus of HDAP2 is not a substrate for biotinidase, so identification of biotin could be used to localize HDAP2 within the tissue.

HDAP2 preserved the mitochondrial membrane potential, limited oxidative stress, and improved cell survival during serum starvation in cultured cells

Mitochondria-promoted cellular oxidative stress is commonly mediated by inhibition of the mitochondrial electron transport chain, which results in a subsequent drop in the mitochondrial membrane potential and accumulation of reactive oxidative species (ROS). In the presence of HDAP2, we did not observe either of these effects. Incubation of MDBK cells with HDAP2 (1 μM) during serum-starvation significantly improved mitochondrial efficiency and cell viability. In serum-starved cultures incubated with MitoTracker Red CMXRos, a mitochondrion-selective dye that accumulates in active mitochondria, fluorescence intensity increased over 2.5 times when cells were treated with HDAP2 compared to untreated controls, demonstrating enhanced mitochondrial membrane potential. The improved potential was accompanied by decreases in oxidative stress measured with the general oxidative stress indicator, CM-

H2DCFDA, which showed >80% reduction in CM-H2DCFDA fluorescence. Confirmation of HDAP2's beneficial action was improved cell survival, which increased by 50% in serum-deprived conditions compared to untreated control cells. While the results are promising, more work is required to determine the mechanism of action of this novel analog.

Survival of retinal ganglion cells

Another important finding from our work was that mitochondrial-directed HDAP2 significantly improved the survival of retinal ganglion cells, at all eccentricities in the retina, following optic nerve crush. The biotinylated peptide was identified in the retina after both intravitreal injection and via systemic administration, demonstrating that water soluble HDAP2 can penetrate the retina-blood barrier and reach mitochondria in retina neurons and glia. Since HDAP2 localizes with known mitochondrial markers, it is likely that the peptide is targeting mitochondria inside animal cells, as it does in cultured cells, to help to improve mitochondrial function. RGCs are among the most metabolically demanding cells in the central nervous system (Wong-Riley, 2010), and they contain correspondingly high concentrations of mitochondria, particularly in unmyelinated intraretinal axons (Wang et al., 2003; Wilkison et al., 2021). Following physical damage to the optic nerve, energy demands on RGCs increase as they attempt to repair axonal damage and reestablish cellular homeostasis. However, as ATP production by mitochondria increases, ROS generation accelerates, which leads to catastrophic cellular effects, including impaired ATP production, mutated mitochondrial DNA, dysregulation of intracellular Ca^{2+}, and activation of apoptotic pathways (Smith et al., 2012). Mitochondria can function normally in the short-term, but over time, cellular

homeostasis is impaired by excessive ROS and leads to mitochondrial dysfunction and death (Sánchez-Migallón et al., 2018).

Increases in RBPMS expression correlates with improved RGC survival

When the intensity of the confocal laser was controlled, the average expression of RBPMS in the HDAP2 treated retinas was double compared to the expression of the label in untreated retinas following ONC. RBPMS selectively labels RGCs in many species (Kwong et al., 2011) and its expression decreases in cells following hypoxia, increased intraocular pressure (Donahue et al., 2021), and after optic nerve crush (Kwong et al., 2011; Pereiro et al., 2020; Rodriguez et al., 2014). These decreases have been correlated with increased expression of caspase 3 (Sánchez-Migallón et al., 2018), a protein that initiates a major apoptotic pathway. When RGC axons are injured, cellular mitochondria experience a drop in the mitochondrial potential, which results in translocation of the pro-apoptotic gene *Bax* (Smaili et al., 2001), induction of mitochondrial permeabilization, and activation of caspase-dependent apoptotic programs (Libby et al., 2005; Raff et al., 2002). BAX can be inhibited by $Bclx_L$ an anti-apoptotic member of the *Bcl2* gene family (Levin et al., 1997) that prevents serum starvation-induced decreases in the mitochondrial membrane potential in cells (Chen et al., 2011; Vander Heiden et al., 1997). When $BCLX_L$ was delivered to animals, it protected the optic nerve and improved RGC survival in DBA/2J mice, who otherwise experienced massive degeneration of RGCs with advancing age. The gene conferred greater protection than genetic deletion of *Bax* alone (Donahue et al., 2021), indicating that preservation of the mitochondrial membrane potential may be a better strategy for protecting RGCs following trauma or disease, than direct prevention of apoptosis.

Impact of retinal eccentricity on RGC survival

HDAP2 improved survival of RGCs at all retinal eccentricities compared to untreated ONC controls but survival was greatest in areas outside central retina (Figure 5B); survival was only 18% greater in central retina compared to 50% greater in peripheral retina ($P<0.0001$). This result is consistent with earlier studies demonstrating that more RGCs survive optic nerve injury when the damage is furthest from the optic nerve head (Bray et al., 1991). Our methodology did not allow us to determine whether ONC disproportionately affected specific subtypes of RGCs, but we did notice that a high fraction of surviving cells had large somas, which suggests they could be alpha RGCs (Figure 4). This observation is consistent with recent studies showing that ON-sustained and ON-transient alpha-ganglion cells are more likely to survive optic nerve crush injury compared to other ganglion cell types (Duan et al., 2015). Interestingly, ON-alpha cells in mouse retina have an uneven distribution with highest densities in peripheral temporal retina, which are the same areas were most protected by the HDAP2 peptide (Bleckert et al., 2014).

The subtype-specific survival of RGCs following ONC may be due to differences in gene activation, variations in the concentration of mitochondria, or retinal eccentricity, but survival could also be dependent on the relative health of Müller cells which also depend heavily on the actions of mitochondria. Müller cells provide essential support to RGCs by delivering nutrients and growth factors, and removing metabolic wastes (Bringmann & Wiedemann, 2011; Eastlake et al., 2021; Seki et al., 2005) also participate in retinal homeostasis by balancing extracellular ion concentrations and neurotransmitters, such as glutamate (Bringmann et al., 2013). Unlike RGCs, which are

most densely concentrated in central retina, Müller cells are homogenously distributed without regard to eccentricity (Wang et al., 2017). With a higher ratio of retinal ganglion cells to Müller cells in central retina, elevated oxidative stress would impact Müller cells in central retina more significantly than those in the periphery, where the workload would be more manageable. HDAP2 labeling was observed in Müller cells (Figure 2) so it is conceivable that improved mitochondrial function as well as higher concentrations of Müller cells in peripheral retina improved RGC survival.

Commercial Relationships

MA MacNeil, None; V Garcia-Marin, None; A Birk**,** None

Figure 1

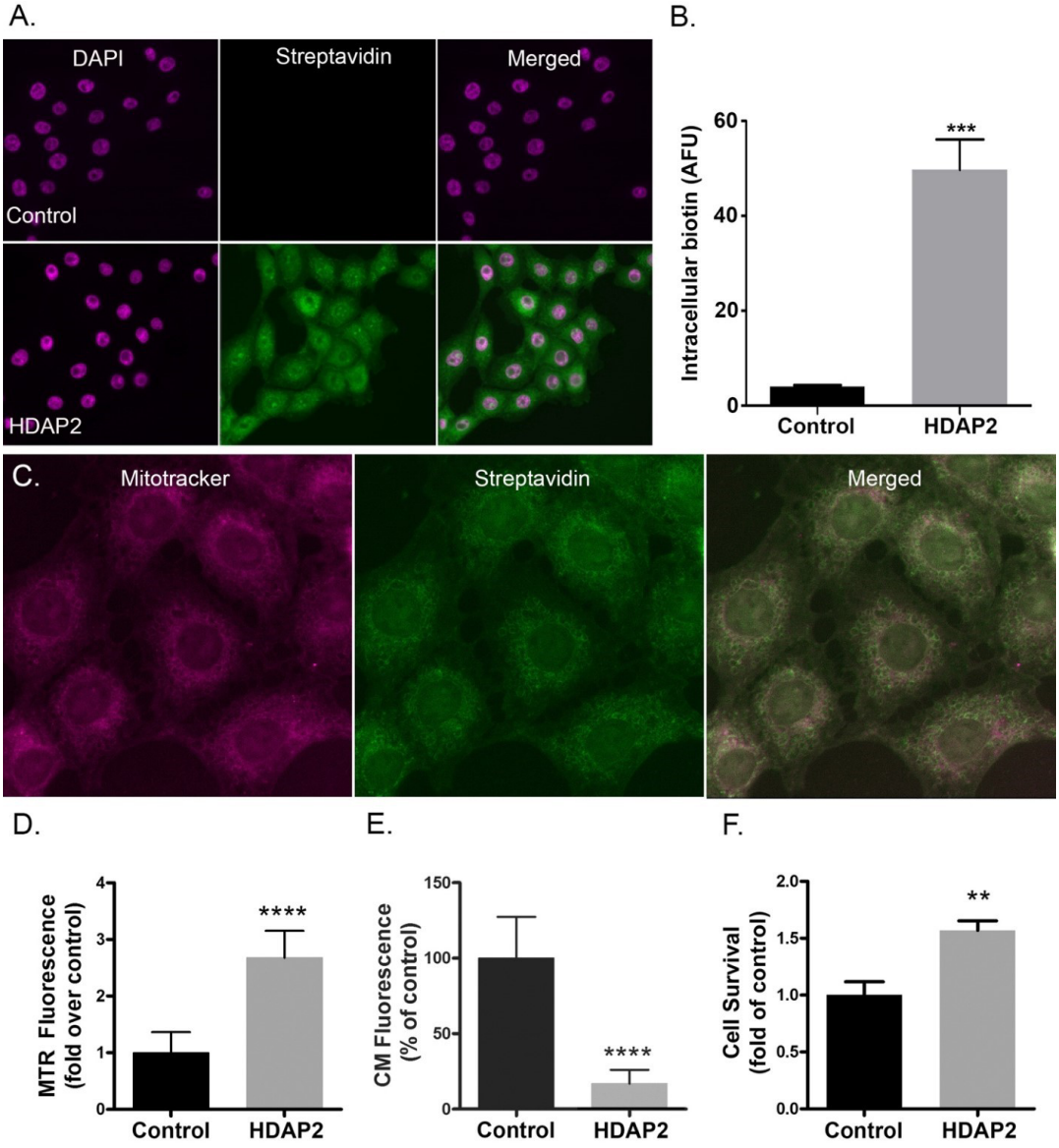

Figure 1: A. Madin-Darby Bovine Kidney (MDBK) cultured cells incubated with DAPI and streptavidin AF 488 to demonstrate that biotinylated HDAP2 readily loads into cells (A) and is expressed at levels far exceeding (>10X) endogenous biotin (B). C. MDBK cells labeled with streptavidin AF488 to identify HDAP2 (green) and MitoTracker Red CMXRos (magenta) to label mitochondria. Co-localization is indicated by the yellow-gray labeling. D-F. Effects of HDAP2 on MDBK cells after 3-4 days of serum starvation. D. HDAP2 improves mitochondrial potential by 2.5-fold. E. HDAP2 decreases fluorescence of CM-H2-DCFDA by 80% compared to control, demonstrating decreases in oxidative stress. F. HDAP2 increased AlamarBlue fluorescence by 50% compared to control, demonstrating that HDAP2 increased cell survival. Differences between Control and HDAP2 -treated conditions were all significantly different from each other (n=5 for each assay; ** $P<0.01$), ***$P<0.001$, and ****$P<0.0001$).

Figure 2

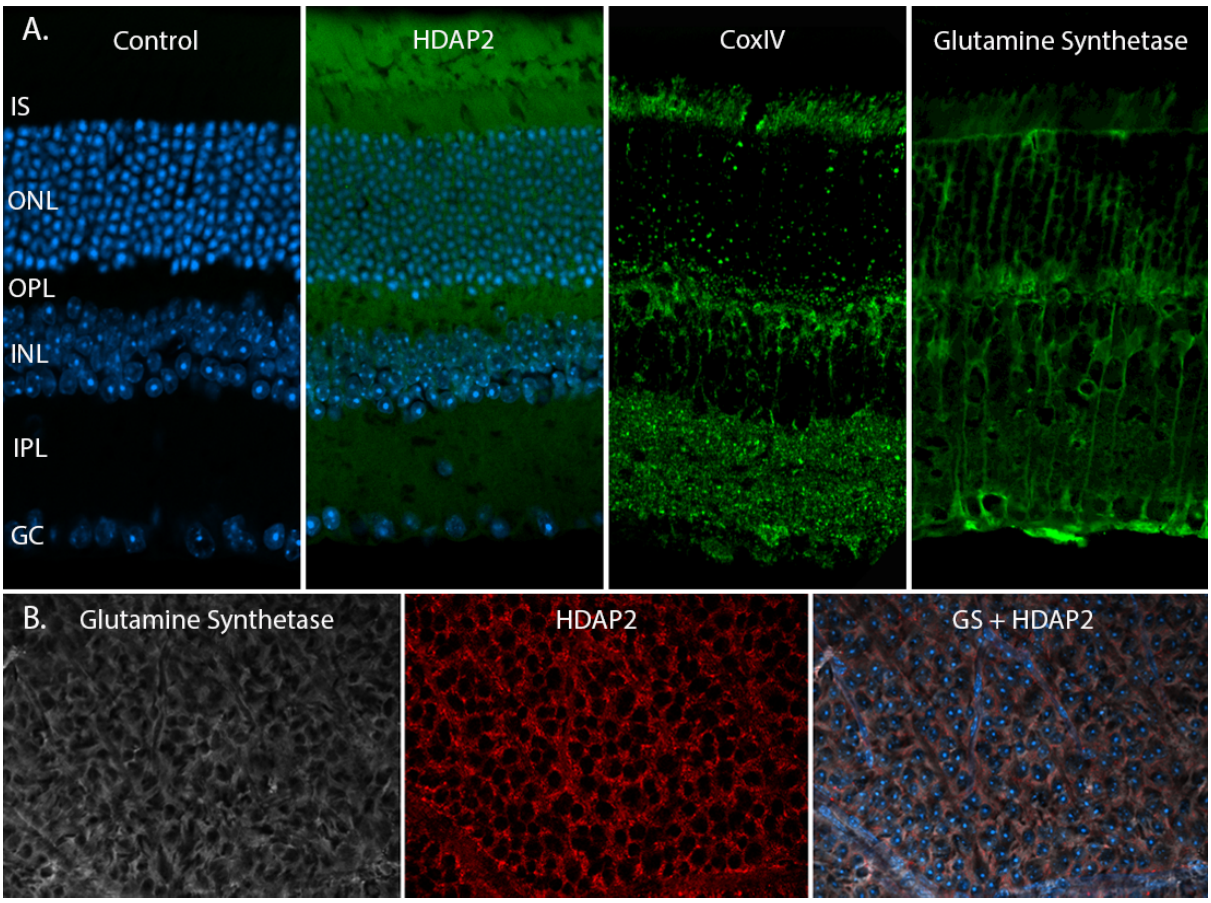

Figure 2: A. Retinal cryostat sections were incubated with streptavidin-conjugated Alexa Fluor 488 to reveal endogenous biotin (Control), biotinylated HDAP2 (HDAP2, green) and ToPro 3 to label cell nuclei (blue). Stained sections were imaged in the confocal microscope using the same PMT voltage to demonstrate relative distribution of the labels. Control sections showed little to no labeling with streptavidin (green), while the HDAP2 exposed animals showed labeling throughout the retina (green), indicating widespread uptake of the peptide. HDAP2 label was distributed similarly to the mitochondrial marker CoxIV, and with glutamine synthetase, a marker for Müller cell glia. B. A triple labeled wholemount with ToPro-stained nuclei in blue, showed HDAP2 colocalized with glutamine synthetase (gray), a high density of HDAP2 labeling alongside blood vessels (red). GC, ganglion cell layer; IPL, inner plexiform layer; INL, inner nuclear layer; OPL, outer plexiform layer; ONL, outer nuclear layer, IS, inner segments of photoreceptors.

Figure 3

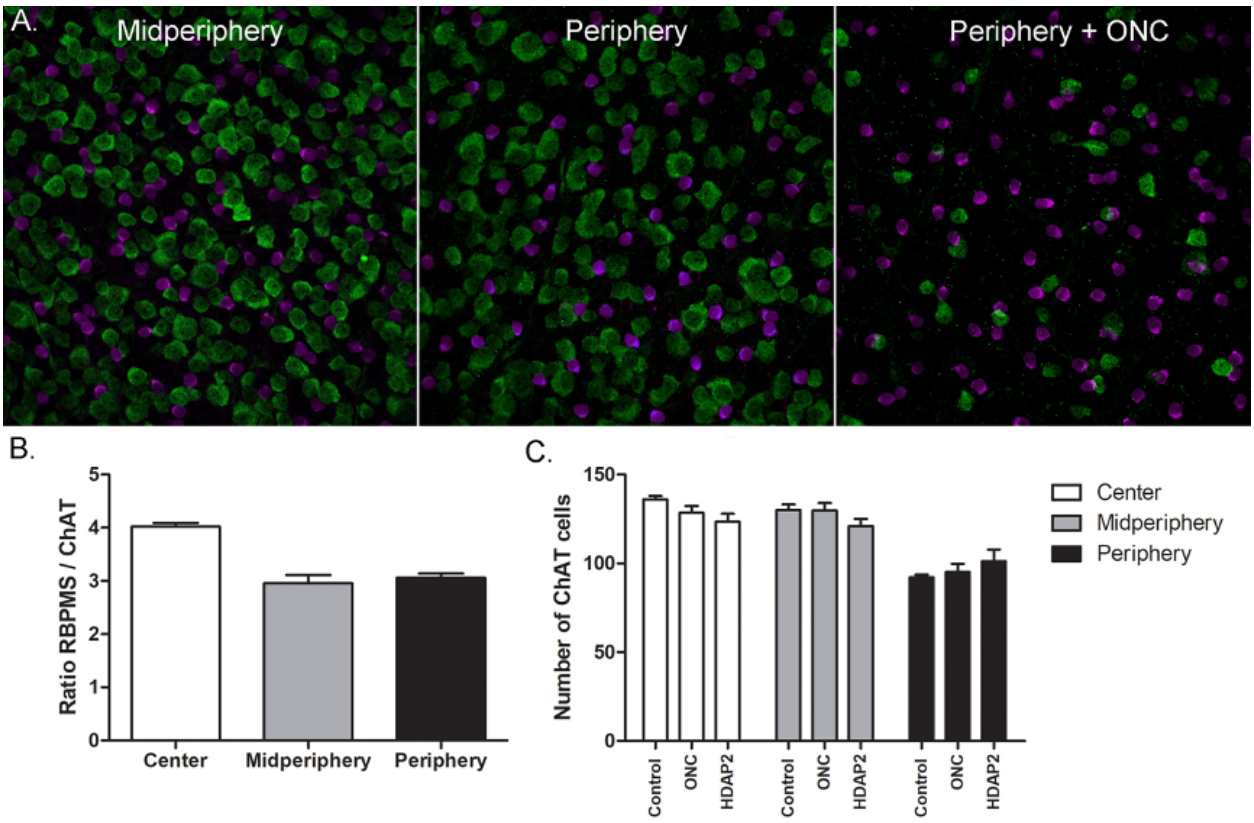

Figure 3: A. Ratios of RGCs labeled with RBPMS (green) and starburst amacrine cells labeled with ChAT (magenta) were used to control for differences in cell density across the retina and to standardize the densities following optic nerve crush (ONC). After ONC, the numbers of RBPMS-labeled neurons decreased significantly, but the distribution of ChAT cells was unaffected. B. Ratios of RBPMS to ChAT was about 4 to 1 in central retina and about 3 to 1 elsewhere. C. The density of ChAT labeled cells in Control, ONC and HDAP2 treatment groups in central, midperipheral and peripheral eccentricities were not significantly different from each other ($P>0.05$, n=11-15 samples per eccentricity), demonstrating their usefulness as an internal control.

Figure 4

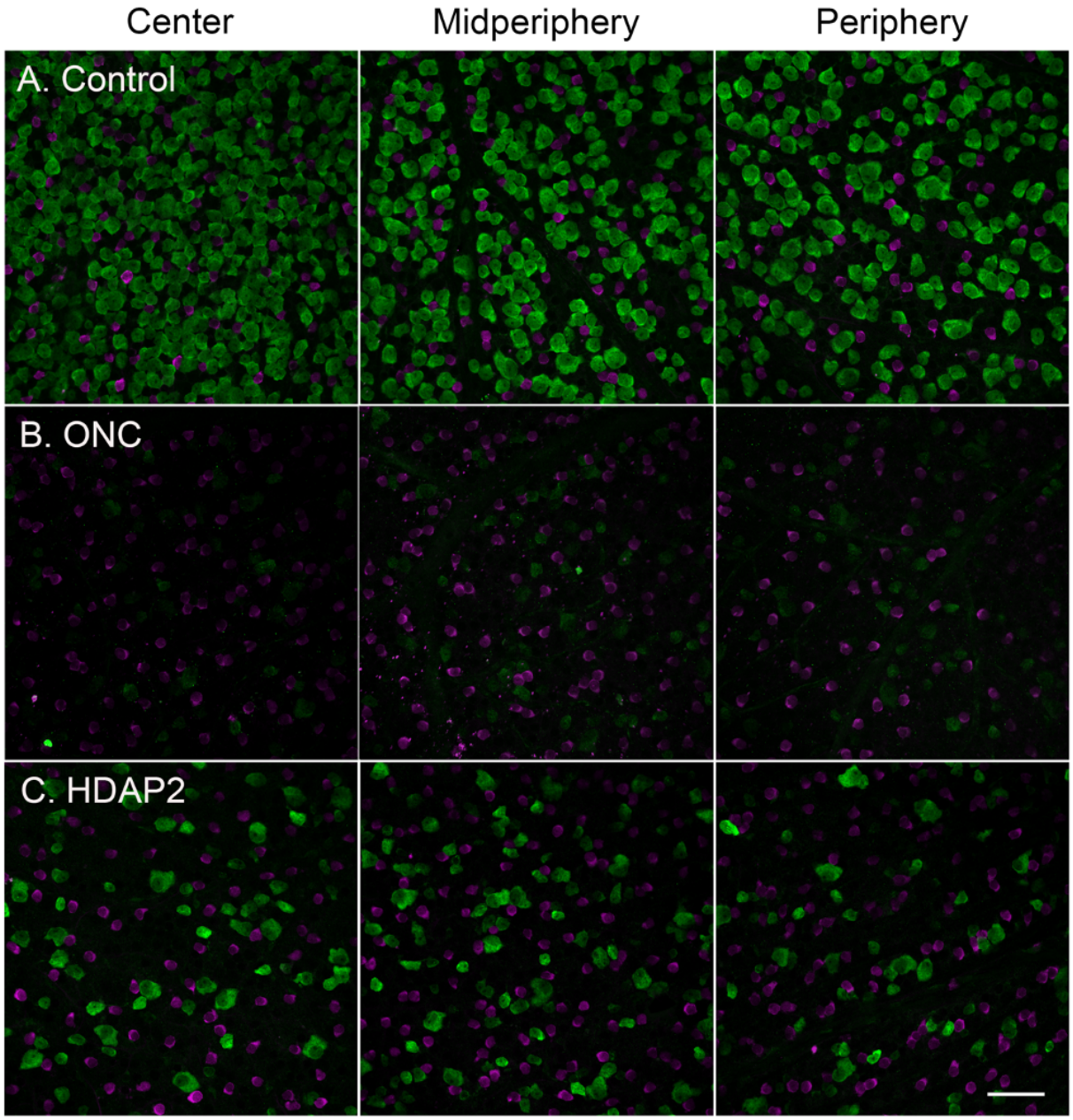

Figure 4: Retinal wholemounts were stained for RGCs (RBPMS, green) and starburst amacrine cells (ChAT, magenta) following optic nerve crush (ONC). The numbers of ChAT-labeled cells were unchanged in all conditions, but ONC induced significant death of RGCs. However, cell survival in HDAP2 treated animals was 40% greater than observed in untreated controls.

Figure 5

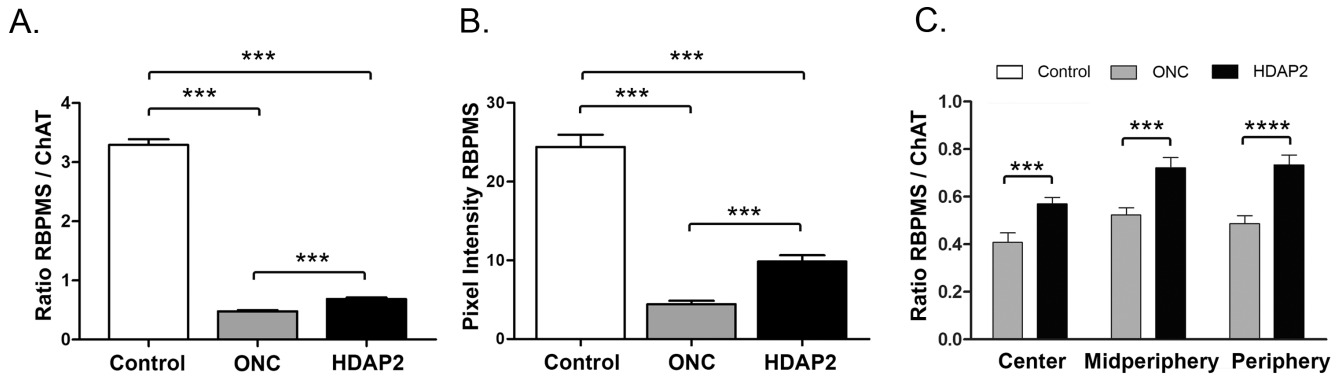

Figure 5. Following ONC, the ratio of RBPMS to ChAT decreased by 80% compared to unoperated control retinas (Fig. 5A, ANOVA, $P<0.001$), but survival of RGCs was significantly greater in HDAP2 treated animals than for the untreated controls at all retinal locations (Fig 5C, Student's t-tests, ****$P<0.0001$, ***$P<0.001$). Expression of RBPMS mirrored these results, showing doubled expression of RBPMS in HDAP2 treated animals compared to untreated controls (Fig. 5B, ANOVA, $P<0.001$).

Table 1: Average density of retinal ganglion cells at varying retinal eccentricity.

	Control	ONC	HDAP2
Central	4465 ± 106.4	408.9 ± 31.21	446.1 ± 42.92
Midperipheral	3070 ± 101.2	490.5 ± 36.77	694.5 ± 52.61
Peripheral	2107 ± 126.6	391.7 ± 35.87	565.4 ± 53.61

The average densities of RBPMS-labeled retina ganglion cells ± SEM, in central, midperipheral and peripheral areas of the retina in control retinas and following optic nerve crush, with and without treatment with HDAP2.

References

Almasieh, M., Wilson, A. M., Morquette, B., Vargas, J. L. C., & Polo, A. D. (2012). The molecular basis of retinal ganglion cell death in glaucoma. *Progress in Retinal and Eye Research*, *31*(2), 152-181. https://doi.org/10.1016/j.preteyeres.2011.11.002 PMID - 22155051

Barron, M. J., Griffiths, P., Turnbull, D. M., Bates, D., & Nichols, P. (2004). The distributions of mitochondria and sodium channels reflect the specific energy requirements and conduction properties of the human optic nerve head. *Br J Ophthalmol*, *88*(2), 286-290. https://doi.org/10.1136/bjo.2003.027664

Birk, A. V., Liu, S., Soong, Y., Mills, W., Singh, P., Warren, D. J., . . . Szeto, H. H. (2013). The mitochondrial-targeted compound SS-31 re-energizes ischemic mitochondria by interacting with cardiolipin. *Journal of the American Society of Nephrology : JASN*, *24*(8), 1250-1261. https://doi.org/10.1681/asn.2012121216

Bleckert, A., Schwartz, G. W., Turner, M. H., Rieke, F., & Wong, R. O. (2014). Visual space is represented by nonmatching topographies of distinct mouse retinal ganglion cell types. *Curr Biol*, *24*(3), 310-315. https://doi.org/10.1016/j.cub.2013.12.020

Bringmann, A., Grosche, A., Pannicke, T., & Reichenbach, A. (2013). GABA and Glutamate Uptake and Metabolism in Retinal Glial (Müller) Cells. *Front Endocrinol (Lausanne)*, *4*, 48. https://doi.org/10.3389/fendo.2013.00048

Bringmann, A., & Wiedemann, P. (2011). Müller Glial Cells in Retinal Disease. *Ophthalmologica*, *227*(1). https://doi.org/10.1159/000328979

Chen, Y. B., Aon, M. A., Hsu, Y. T., Soane, L., Teng, X., McCaffery, J. M., . . . Hardwick, J. M. (2011). Bcl-xL regulates mitochondrial energetics by stabilizing the inner membrane potential. *J Cell Biol*, *195*(2), 263-276. https://doi.org/10.1083/jcb.201108059

Chrysostomou, V., Rezania, F., Trounce, I. A., & Crowston, J. G. (2013). Oxidative stress and mitochondrial dysfunction in glaucoma. *Current Opinion in Pharmacology*, *13*(1), 12-15. https://doi.org/10.1016/j.coph.2012.09.008 PMID - 23069478

Crish, S. D., Sappington, R. M., Inman, D. M., Horner, P. J., & Calkins, D. J. (2010). Distal axonopathy with structural persistence in glaucomatous neurodegeneration. *Proc Natl Acad Sci U S A*, *107*(11), 5196-5201. https://doi.org/10.1073/pnas.0913141107

Donahue, R. J., Fehrman, R. L., Gustafson, J. R., & Nickells, R. W. (2021). BCLXL gene therapy moderates neuropathology in the DBA/2J mouse model of inherited glaucoma. *Cell Death & Disease*, *12*(8), 781. https://doi.org/10.1038/s41419-021-04068-x PMID - 34376637

Duan, X., Qiao, M., Bei, F., Kim, I. J., He, Z., & Sanes, J. R. (2015). Subtype-specific regeneration of retinal ganglion cells following axotomy: effects of osteopontin and mTOR signaling. *Neuron*, *85*(6), 1244-1256. https://doi.org/10.1016/j.neuron.2015.02.017

Eastlake, K., Lamb, W. D. B., Luis, J., Khaw, P. T., Jayaram, H., & Limb, G. A. (2021). Prospects for the application of Müller glia and their derivatives in retinal regenerative therapies. *Prog Retin Eye Res*, *85*, 100970. https://doi.org/10.1016/j.preteyeres.2021.100970

Galindo-Romero, C., Avilés-Trigueros, M., Jiménez-López, M., Valiente-Soriano, F. J., Salinas-Navarro, M., Nadal-Nicolás, F., . . . Agudo-Barriuso, M. (2011). Axotomy-induced retinal ganglion cell death in adult mice: quantitative and topographic time course analyses. *Exp Eye Res*, *92*(5), 377-387. https://doi.org/10.1016/j.exer.2011.02.008

Hou, M., Shao, Z., Zhang, S., Liu, X., Fan, P., Jiang, M., . . . Yuan, H. (2022). Age-related visual impairments and retinal ganglion cells axonal degeneration in a mouse model harboring OPTN (E50K) mutation. *Cell Death Dis*, *13*(4), 362. https://doi.org/10.1038/s41419-022-04836-3

Ito, Y. A., & Polo, A. D. (2017). Mitochondrial dynamics, transport, and quality control: A bottleneck for retinal ganglion cell viability in optic neuropathies. *Mitochondrion*, *36*, 186-192. https://doi.org/10.1016/j.mito.2017.08.014 PMID - 28866056

Jakobs, T. C., Libby, R. T., Ben, Y., John, S., & Masland, R. H. (2005). Retinal ganglion cell degeneration is topological but not cell type specific in DBA/2J mice. *The Journal of Cell Biology*, *171*(2), 313-325. https://doi.org/10.1083/jcb.200506099 PMID - 16247030

Jassim, A. H., Inman, D. M., & Mitchell, C. H. (2021). Crosstalk Between Dysfunctional Mitochondria and Inflammation in Glaucomatous Neurodegeneration. *Front Pharmacol*, *12*, 699623. https://doi.org/10.3389/fphar.2021.699623

Jeena, M. T., Palanikumar, L., Go, E. M., Kim, I., Kang, M. G., Lee, S., . . . Ryu, J. H. (2017). Mitochondria localization induced self-assembly of peptide amphiphiles for cellular dysfunction. *Nat Commun*, *8*(1), 26. https://doi.org/10.1038/s41467-017-00047-z

Kalesnykas, G., Oglesby, E. N., Zack, D. J., Cone, F. E., Steinhart, M. R., Tian, J., . . . Quigley, H. A. (2012). Retinal ganglion cell morphology after optic nerve crush and experimental glaucoma. *Invest Ophthalmol Vis Sci*, *53*(7), 3847-3857. https://doi.org/10.1167/iovs.12-9712

Kong, G. Y. X., Bergen, N. J. V., Trounce, I. A., & Crowston, J. G. (2009). Mitochondrial Dysfunction and Glaucoma. *Journal of Glaucoma*, *18*(2), 93-100. https://doi.org/10.1097/ijg.0b013e318181284f PMID - 19225343

Kwong, J. M., Quan, A., Kyung, H., Piri, N., & Caprioli, J. (2011). Quantitative analysis of retinal ganglion cell survival with Rbpms immunolabeling in animal models of optic neuropathies. *Invest Ophthalmol Vis Sci*, *52*(13), 9694-9702. https://doi.org/10.1167/iovs.11-7869

Levin, L. A., Schlamp, C. L., Spieldoch, R. L., Geszvain, K. M., & Nickells, R. W. (1997). Identification of the bcl-2 family of genes in the rat retina. *Invest Ophthalmol Vis Sci*, *38*(12), 2545-2553.

Libby, R. T., Li, Y., Savinova, O. V., Barter, J., Smith, R. S., Nickells, R. W., & John, S. W. (2005). Susceptibility to neurodegeneration in a glaucoma is modified by Bax gene dosage. *PLoS Genet*, *1*(1), 17-26. https://doi.org/10.1371/journal.pgen.0010004

Lin, M. T., & Beal, F. M. (2006). Mitochondrial dysfunction and oxidative stress in neurodegenerative diseases. *Nature*, *443*(7113), 787-795. https://doi.org/10.1038/nature05292

Liu, H., & Prokosch, V. (2021). Energy Metabolism in the Inner Retina in Health and Glaucoma. *Int J Mol Sci*, *22*(7). https://doi.org/10.3390/ijms22073689

Marchesan, S., Vargiu, A. V., & Styan, K. E. (2015). The Phe-Phe Motif for Peptide Self-Assembly in Nanomedicine. *Molecules*, *20*(11), 19775-19788. https://doi.org/10.3390/molecules201119658

Mazzio, E. A., & Soliman, K. F. (2004). Effects of enhancing mitochondrial oxidative phosphorylation with reducing equivalents and ubiquinone on 1-methyl-4-phenylpyridinium toxicity and complex I-IV damage in neuroblastoma cells. *Biochem Pharmacol*, *67*(6), 1167-1184. https://doi.org/10.1016/j.bcp.2003.11.016

Mead, B., Thompson, A., Scheven, B. A., Logan, A., Berry, M., & Leadbeater, W. (2014). Comparative evaluation of methods for estimating retinal ganglion cell loss in retinal sections and wholemounts. *PloS one*, *9*(10), e110612. https://doi.org/10.1371/journal.pone.0110612 PMID - 25343338

Murphy, M. (2016). Understanding and preventing mitochondrial oxidative damage.

Nadal-Nicolás, F. M., Sobrado-Calvo, P., Jiménez-López, M., Vidal-Sanz, M., & Agudo-Barriuso, M. (2015). Long-Term Effect of Optic Nerve Axotomy on the Retinal Ganglion Cell Layer. *Invest Ophthalmol Vis Sci*, *56*(10), 6095-6112. https://doi.org/10.1167/iovs.15-17195

Nascimento-Dos-Santos, G., de-Souza-Ferreira, E., Lani, R., Faria, C. C., Araujo, V. G., Teixeira-Pinheiro, L. C., . . . Petrs-Silva, H. (2020). Neuroprotection from optic nerve injury and modulation of oxidative metabolism by transplantation of active mitochondria to the retina. *Biochim Biophys Acta Mol Basis Dis*, *1866*(5), 165686. https://doi.org/10.1016/j.bbadis.2020.165686

Nathanael, J. G., Gamon, L. F., Cordes, M., Rablen, P. R., Bally, T., Fromm, K. M., . . . Wille, U. (2018). Amide Neighbouring-Group Effects in Peptides: Phenylalanine as Relay Amino Acid in Long-Distance Electron Transfer. *Chembiochem*, *19*(9), 922-926. https://doi.org/10.1002/cbic.201800098

Nickells, R. W., Howell, G. R., Soto, I., & John, S. W. M. (2012). Under Pressure: Cellular and Molecular Responses During Glaucoma, a Common Neurodegeneration with Axonopathy. *Annual review of neuroscience*, *35*(1), 153-179. https://doi.org/10.1146/annurev.neuro.051508.135728

Nunnari, J., & Suomalainen, A. (2012). Mitochondria: In Sickness and in Health. *Cell*, *148*(6), 1145-1159. https://doi.org/10.1016/j.cell.2012.02.035

Pereiro, X., Ruzafa, N., Urcola, H. J., Sharma, S. C., & Vecino, E. (2020). Differential Distribution of RBPMS in Pig, Rat, and Human Retina after Damage.

Raff, M. C., Whitmore, A. V., & Finn, J. T. (2002). Axonal self-destruction and neurodegeneration. *Science*, *296*(5569), 868-871. https://doi.org/10.1126/science.1068613

Rodriguez, A. R., de Sevilla Müller, L. P., & Brecha, N. C. (2014). The RNA binding protein RBPMS is a selective marker of ganglion cells in the mammalian retina. *J Comp Neurol*, *522*(6), 1411-1443. https://doi.org/10.1002/cne.23521

Samuel, M. A., Zhang, Y., Meister, M., & Sanes, J. R. (2011). Age-related alterations in neurons of the mouse retina. *J Neurosci*, *31*(44), 16033-16044. https://doi.org/10.1523/JNEUROSCI.3580-11.2011

Schrier, S. A., & Falk, M. J. (2011). Mitochondrial disorders and the eye. *Curr Opin Ophthalmol*, *22*(5), 325-331. https://doi.org/10.1097/ICU.0b013e328349419d

Seki, M., Tanaka, T., Sakai, Y., Fukuchi, T., Abe, H., Nawa, H., & Takei, N. (2005). Müller Cells as a source of brain-derived neurotrophic factor in the retina: noradrenaline upregulates brain-derived neurotrophic factor levels in cultured rat Müller cells. *Neurochem Res*, *30*(9), 1163-1170. https://doi.org/10.1007/s11064-005-7936-7

Smaili, S. S., Hsu, Y. T., Sanders, K. M., Russell, J. T., & Youle, R. J. (2001). Bax translocation to mitochondria subsequent to a rapid loss of mitochondrial membrane potential. *Cell Death Differ*, *8*(9), 909-920. https://doi.org/10.1038/sj.cdd.4400889

Smith, R. A. J., Hartley, R. C., Cochemé, H. M., & Murphy, M. P. (2012). Mitochondrial pharmacology. *Trends in Pharmacological Sciences*, *33*(6), 341-352. https://doi.org/10.1016/j.tips.2012.03.010 PMID - 22521106

Sánchez-Migallón, M. C., Valiente-Soriano, F. J., Salinas-Navarro, M., Nadal-Nicolás, F. M., Jiménez-López, M., Vidal-Sanz, M., & Agudo-Barriuso, M. (2018). Nerve fibre layer degeneration and retinal ganglion cell loss long term after optic nerve crush or transection in adult mice. *Exp Eye Res*, *170*, 40-50. https://doi.org/10.1016/j.exer.2018.02.010

Tang, Z., Zhang, S., Lee, C., Kumar, A., Arjunan, P., Li, Y., . . . Li, X. (2011). An Optic Nerve Crush Injury Murine Model to Study Retinal Ganglion Cell Survival. *Journal of Visualized Experiments*(50). https://doi.org/10.3791/2685

Tao, K., Makam, P., Aizen, R., & Gazit, E. (2017). Self-assembling peptide semiconductors. *Science*, *358*(6365). https://doi.org/10.1126/science.aam9756

Tribble, J. R., Otmani, A., Sun, S., Ellis, S. A., Cimaglia, G., Vohra, R., . . . Williams, P. A. (2021). Nicotinamide provides neuroprotection in glaucoma by protecting against mitochondrial and metabolic dysfunction. *Redox Biology*, *43*, 101988. https://doi.org/10.1016/j.redox.2021.101988 PMID - 33932867

Vander Heiden, M. G., Chandel, N. S., Williamson, E. K., Schumacker, P. T., & Thompson, C. B. (1997). Bcl-xL regulates the membrane potential and volume homeostasis of mitochondria. *Cell*, *91*(5), 627-637. https://doi.org/10.1016/s0092-8674(00)80450-x

Wang, J., O'Sullivan, M. L., Mukherjee, D., Puñal, V. M., Farsiu, S., & Kay, J. N. (2017). Anatomy and spatial organization of Müller glia in mouse retina. *J Comp Neurol*, *525*(8), 1759-1777. https://doi.org/10.1002/cne.24153

Wang, L., Dong, J., Cull, G., Fortune, B., & Cioffi, G. A. (2003). Varicosities of intraretinal ganglion cell axons in human and nonhuman primates. *Invest Ophthalmol Vis Sci*, *44*, 2-9.

Wilkison, S. J., Bright, C. L., Vancini, R., Song, D. J., Bomze, H. M., & Cartoni, R. (2021). Local Accumulation of Axonal Mitochondria in the Optic Nerve Glial Lamina Precedes Myelination. *Front Neuroanat*, *15*, 678501. https://doi.org/10.3389/fnana.2021.678501

Williams, P. A., Harder, J. M., & John, S. (2017). Glaucoma as a Metabolic Optic Neuropathy. *Journal of Glaucoma*, *26*(12), 1161-1168. https://doi.org/10.1097/IJG.0000000000000767

Williams, P. R., Benowitz, L. I., Goldberg, J. L., & He, Z. (2020). Axon Regeneration in the Mammalian Optic Nerve. *Annu Rev Vis Sci*, *6*, 195-213. https://doi.org/10.1146/annurev-vision-022720-094953

Wong-Riley, M. T. (2010). Energy metabolism of the visual system. *Eye Brain*, *2*, 99-116. https://doi.org/10.2147/EB.S9078

Yu Wai Man, C. Y., Chinnery, P. F., & Griffiths, P. G. (2005). Optic neuropathies--importance of spatial distribution of mitochondria as well as function. *Med Hypotheses*, *65*(6), 1038-1042. https://doi.org/10.1016/j.mehy.2004.10.021

Zhao, K., Zhao, G. M., Wu, D., Soong, Y., Birk, A. V., Schiller, P. W., & Szeto, H. H. (2004). Cell-permeable peptide antioxidants targeted to inner mitochondrial membrane inhibit mitochondrial swelling, oxidative cell death, and reperfusion injury. *J Biol Chem*, *279*(33), 34682-34690. https://doi.org/10.1074/jbc.M402999200